Propagation Based Spectrum Sensing: A Novel Beamforming Detection Method

Jonathan S. Lu and I-Tai Lu
Department of Electrical and Computer Engineering, Polytechnic Institute of NYU
6 MetroTech, Brooklyn, NY, 11201, USA
lushiaoen@gmail.com, itailu@poly.edu

***Abstract*—This paper proposes a novel propagation based spectrum sensing method that utilizes beamforming for systems equipped with antenna arrays. Since rays are known to arrive in clusters, the arrival angles of the dominant ray clusters can be exploited to improve the spectral sensing performances. Moreover, from site-specific propagation characteristics, the dominant ray angles can be predicted without additional computational efforts in most practical environments. Numerical results based on ray-based channel models show that the proposed beamforming detection method (with or without dominant ray angle prediction) is superior to the conventional energy detection method. Numerical results also show that decreasing the angle spread, enhances the performance of the proposed method. The computational complexity and latency of the proposed method is the same as the conventional energy detection method when using dominant ray angle prediction, but increases slightly without prediction.**

Keywords-component; Angle of Arrival, Beamforming, Cognitive Radio, Dominant Ray, Propagation Site-specific, Spectrum Sensing.

I. INTRODUCTION

Cognitive Radio utilizes opportunistic spectrum access to allow for a greater number of users. It enables secondary users to make use of the unused spectrum in the pre-allocated bands for primary users (e.g., see [1, 2]). These secondary users may find opportunities to communicate in frequency, time, geographical space, code and angle [1]. To fully utilize these opportunities, a robust spectrum sensing method must be employed to test whether the spectrum in question is available.

Spectrum sensing can be divided into feature based and non-feature based sensing [1]. Feature based sensing takes advantage of the features of the primary user's signal. Some examples are cyclostationary based (e.g., see [3]) and waveform based sensing (e.g., see [4]). Cyclostationary based sensing utilizes the periodicity of the signal and signal statistics such as mean and autocorrelation. Waveform based sensing utilizes the known signal patterns in wireless systems. A non-feature based sensing method is energy detection (e.g., see [5]), but its major drawback is a sensitivity to noise uncertainty.

In [6], propagation issues for cognitive radio are surveyed, but to the best of our knowledge, propagation features have not been taken advantage of in spectrum sensing. We propose in this paper to exploit propagation features (specifically the angles of dominant arrivals) for spectral sensing. To do so, a multiple antenna setup is required. Note that multiple antennas have been employed for cooperative sensing, in which they cooperate to make decisions on whether a primary user is present. Advantages of cooperative sensing are a greater resilience to noise uncertainty and fast fading [1]. In data fusion, a type of cooperative sensing where antennas are spaced far apart, the received signals are generally considered uncorrelated and many schemes have been proposed to combine the data from each antenna non-coherently [7]. If an antenna array is employed, the antennas may be correlated. In [8, 9], the antenna correlation is utilized for spectral sensing based on statistical channel models. Consequently, propagation characteristics are not taken advantage of.

This paper proposes a novel beamforming detection method to exploit the propagation characteristic of rays arriving in clusters. This characteristic has been well documented and is seen in measurements of the radio channel [10, 11]. In some propagation scenarios, the arrival angles of the dominant ray clusters can be predicted without additional computation efforts based on site-specific propagation characteristics. In all other scenarios, angles of arrivals have to be searched for.

Both ray-based and statistical channel models are used to assess the effectiveness of the proposed beamforming method. This is because a ray-based channel model (as depicted in Fig. 1) has greater accuracy in portraying the site-specific propagation characteristics, while a statistical model is more convenient for characterizing the spatial and/or time correlations. Note that the statistical model does not account for propagation characteristics explicitly and therefore cannot be used to model site-specific propagation accurately.

In Section II, the ray-based and statistical channel models, and the energy and beamforming detectors are derived. The site-specific ray characterizations are summarized in Section III for both cellular and mobile-to-mobile (MTM) communications in rural and urban environments. Results and analyses for simulations that mimic these environments and utilize energy and beamforming detection spectrum sensing methods are presented in Section IV. Conclusions are drawn in Section V.

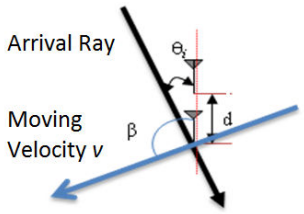

Fig. 1 A moving antenna array.

II. FORMULATION

Consider a uniform linear array with M receiving antennas to detect a primary signal with carrier frequency f_c as seen in Figure 1. The linear array is moving with a constant speed v. Let the angle between the moving direction and the orientation (i.e., end fire direction) of the linear array be β and d be the spacing between two adjacent antennas. Also let C denote the speed of light and λ (=C/f_c) denote the wavelength. The received signal y_m, m=1,2,…,M, at the m^{th} antenna can be expressed as

$$y_m(t) = \alpha h_m(t)s(t) + n_m(t), \tag{1}$$

where h_m is the channel response and n_m is the additive zero-mean white Gaussian noise. A flat fading channel is assumed and $s(t)$ is the transmitted narrowband signal. In (1), α =1 if the primary signal is present and is zero otherwise. The spatial correlation of the received signal is given as

$$R_{yy,ml} \triangleq E\{y_m(t)y_l^*(t)\} \approx \frac{1}{Q}\sum_{q=1}^{Q} y_m(q\Delta t)y_l^*(q\Delta t), \tag{2}$$

where m and l denote the m^{th} and l^{th} antennas in the antenna array, Δt is the sampling interval and $Q\Delta t$ is the total observation time. The approximation in (2) is valid only when the corresponding process is ergodic and both Δt and Q are appropriately chosen. Note that the energy received at the m^{th} receiver antenna is $R_{yy,mm}$.

A. Ray-Based Channel Model

If there are I rays, the channel response is represented as

$$h_m(t) = \sum_{i=1}^{I} a_i \exp\left\{-2\pi j\left[(m-1)\frac{d}{\lambda}\cos\theta_i + f_i t\right]\right\}, \tag{3}$$

where a_i, θ_i and f_i are the complex amplitude, arriving angle and Doppler frequency shift of the i^{th} rays. The Doppler frequency shift can be written as

$$f_i = f_D\cos(\theta_i - \beta), \quad f_D = f_c\frac{v}{C} \tag{4}$$

where f_D is the maximum Doppler spread.

B. Statistical Channel Model

Without loss of generality, the channel response $h_m(t)$ is assumed to be a complex Gaussian random process with zero mean and σ^2 variance. The spatial correlation between the channel responses at the m^{th} and l^{th} antennas is

$$R_{hh,ml}(0) \triangleq E\{h_m(t)h_l^*(t)\} = \sigma^2\rho^{|m-l|}, \ \forall m,l = 1,...,M \tag{5}$$

where ρ is the antenna correlation coefficient between adjacent antennas in the receiving antenna array. The time correlation between the channel responses at time t_1 and time t_2=t_1+t is

$$R_{hh}(t = t_2 - t_1) \triangleq E\{h_m(t_1)h_m^*(t_2)\} = \sigma^2 e^{\frac{-|t_1-t_2|}{T}}, \ \forall m = 1,...,M \tag{6}$$

where T is a time constant.

C. Energy Detection

The conventional energy detector is implemented as follows:

$$H_0 : \frac{1}{M}\sum_{m=1}^{M} R_{yy,mm} \le \eta; \quad \text{primary signal is not detected} \tag{7a}$$

$$H_1 : \frac{1}{M}\sum_{m=1}^{M} R_{yy,mm} > \eta; \quad \text{the primary signal is detected} \tag{7b}$$

where η is the threshold.

D. Beamforming

A conventional beamformer is

$$\bar{y}_\phi(t) = \frac{1}{\sqrt{M}}\sum_{m=1}^{M} y_m(t)\exp\left[j2\pi(m-1)\frac{d}{\lambda}\cos\phi\right] \tag{8}$$

where ϕ denotes the beamforming direction. The Angle correlation of beamformings at ϕ and φ is given by

$$R_{\bar{y}\bar{y},\phi\varphi} \triangleq E\{\bar{y}_\phi(t)\bar{y}_\varphi^*(t)\} \approx \frac{1}{Q}\sum_{q=1}^{Q}\bar{y}_\phi(q\Delta t)\bar{y}_\varphi^*(q\Delta t), \tag{9}$$

with the same assumptions of ergodicity and appropriate Δt and Q. The beamforming detector is

$$H_0 : \max_{\phi}\left\{R_{\bar{y}\bar{y},\phi\phi}\right\} \le \gamma, \quad \text{primary signal is not detected} \tag{10a}$$

$$H_1 : \max_{\phi}\left\{R_{\bar{y}\bar{y},\phi\phi}\right\} > \gamma, \quad \text{primary signal is detected} \tag{10b}$$

where γ is the threshold.

III. APPLICATIONS AND SITE SPECIFIC CHANNEL MODELS

Wave propagation characteristics depend heavily on the height of the transmitting and receiving antennas relative to the surrounding buildings or objects in the vicinity. For convenience, we characterize a communication link as line-of-sight (LOS) or non-line-of-sight (NLOS) by the visibility between the transmitter (Tx) and receiver (Rx) antennas. For LOS links, the dominant rays are a direct ray and possibly a ground reflected ray [11, 12]. Therefore the predicted direction of arrival is in the direction of Tx. The channel response will be modeled by a strong ray cluster with some other weak rays. Here, the angle of the strong ray arrival is known and is set to be zero. The remaining section will be devoted to discussions of scenarios with NLOS links.

A. Cellular Communications

In macro-cellular cells, the transmitting antenna is high above the rooftops in urban environments or is higher than the surrounding objects in rural environments. In micro-cellular cells, the antenna is usually near the building heights. It is thought to be difficult to predict the dominant ray paths for links in typical macro-cellular and micro-cellular cells, but measurements in [11] show that in some NLOS scenarios, dominant rays travel along the streets. In this paper, the channel response for our numerical simulations will be modeled by summing over a random number of ray clusters.

B. MTM Communications

MTM communications are implemented and used in military communication systems and ad-hoc networks. Note that MTM communications are characterized by low transmitting and receiving antenna heights. Depending on the type of environment and the type of link, the dominant rays can be characterized to travel on specific paths in urban and rural environments.

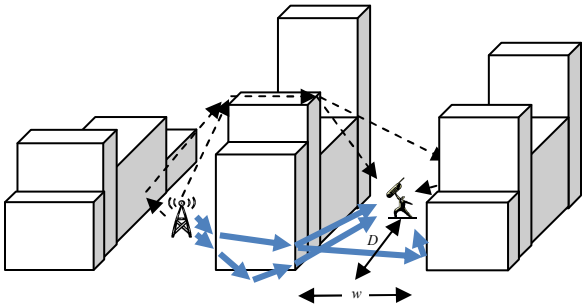

Fig. 2 Ray Paths in an Urban Environment

Urban environments can be further categorized as low-rise buildings, high-rise buildings or a combination of the two. In [13], simulations have shown that the transition from low-rise to high-rise building environments occurs from 9 m to 18 m or 3 stories to 6 stories (1 story = 3 m). Environments with average building height below this region can be considered low-rise and above this region can be considered high-rise.

1) Low-rise Urban Environments

In the case of low-rise building environments, the mobiles are very close to the average building height, so rays in or close to the vertical plane containing the mobiles, depicted by dashed lines in Fig. 2, will frequently give the dominant contribution [14]. Therefore rays will arrive from the direction of Tx. The channel response will be modeled by a strong ray cluster with some other weak rays. However, the angle of the strong arrival is not necessarily known.

2) High-rise Urban Environments

In the case of high-rise building environments, the mobiles are far from the building heights. The dominant contribution to received power often comes from rays that propagate in the street canyons, depicted by solid lines in Fig. 2, by diffracting at the building edges of the intersections [15], scattering from long vertical objects [16] and reflecting off of the buildings lining the street. These rays will arrive at different angles, but it is expected that the diffraction from the corners and scattering from objects like lamppost located at the corners will give the dominant rays. If the width of the street is w and the receiver distance from the intersection is D, the total range of angles is

$$\theta_{range} = 2\tan^{-1}\left(\frac{w/2}{D}\right) . \qquad (11)$$

If D is much larger than w/2, θ_{range} is small. Thus, rays turning at an intersection are expected to arrive in a cluster. Assuming an ideal environment where the blocks are in uniform rectangular shapes, dominant rays may arrive from along the street on either or both sides of the antenna array. Thus, the channel response will be modeled by two strong ray clusters with some other weak rays. The angles of these two strong ray arrivals are known and are set to be zero and π, respectively.

3) Rural Environments

The TIREM model is well accepted in computing the small area average path gain in rural mountainous environments [17]. It only looks at the terrain profile in the vertical plane containing Tx and Rx, so it is expected that the dominant rays, similar to urban low-rise environments, will arrive from the direction of the mobile. Thus, the channel response will be modeled by a strong ray cluster with some other weak rays. However, the angle the strong ray arrival is not necessarily known.

IV. Simulations and Analysis

Simulations are made to mimic different environments discussed in Section III. For each simulation, a total number of 200 realizations of channels were done to calculate false alarm rate (probability of the event that signal was detected, but is not present; $P(H_1|H_0)$) and the missing packet rate (probability of the event that signal was not detected but is present; $P(H_0|H_1)$). For each channel realization, 5000 samples are made in 5 ms, the number of antennas M is either 2 or 4, and the receive SNR of instantaneous power is -20dB. In each case, false alarm rate versus missing pack rate is plotted over the whole ranges of thresholds η in (7) and γ in (10).

A. Ray-Based Channel Simulations

To generate the channel response in (3), the antenna array is oriented with the mobile moving direction (β=0), the maximum Doppler spread is 100Hz, the antenna spacing is half wavelength and the angle spread of each ray cluster is around 10 degrees ($w/D \approx 0.175$).

Along with the energy detection curve, there are two types of beamforming. When the arrival angle of the dominant ray is not known, the beamforming in (8) will be performed over twelve ϕ angles (in between 0 and π) and the angle with the largest beamforming energy will be selected to perform the spectral sensing test in (10). This result will be denoted as *Beamforming*. On the other hand, when the arrival angle of the dominant ray is predicted, the beamforming energy at that particular angle will be used to perform the spectral sensing test in (10). This result will be denoted as *Peak BF*.

Fig. 3 shows results for environments with one strong ray cluster. When the angle of the strong arrival is known (*Peak BF*), the scenario represents the LOS links for both cellular and MTM communications in all environments. When the angle is not known (*Beamforming*), the scenario represents the NLOS links for MTM communications in low-rise urban or rural environments. Fig. 4 shows results for environments with two strong ray clusters. When the angles of the two strong arrivals are known (*Peak BF*), the scenario represents the NLOS links for MTM communications in high-rise urban environments. When the two angles are not known (*Beamforming*), the propagation scenario, may be seen in micro-cellular communications when there can be a rooftop diffracted ray and a rooftop diffracted then reflected ray. Fig. 5 shows results for environments with six strong ray clusters. Fig. 6 shows results for environments with many uniformly distributed ray clusters. The *Beamforming* scenarios in both Figs. 5 and 6 represent possible NLOS links for cellular communications in both macro and micro cells. The *Peak BF* scenarios in both Figs. 5 and 6 are not typical and are not discussed in Section III.

B. Statistical Channel Simulations

For the statistical channel models, the normalized spatial correlations (ρ in (5)) are 0.2 and 0.8 for Figs. 7 and 8, respectively. The time constant T in (6) is 0.1.

C. Analysis

When the number of antennas increases in Figs. 3-8, the missing packet rate and false alarm rate decrease for all methods. This result shows the obvious benefits of a multiple antenna receiver.

For the ray-based channel model results (Fig. 3-6), the two beamforming detection approaches (*Peak BF* and *Beamforming*) are clearly better than *Energy* detection for scenarios where dominant rays arrive in a few clusters. When the angle of the dominant ray cluster can be predicted, the *Peak BF* outperforms *Beamforming*. As the number of ray clusters increase or equivalently angle spread increases, *Peak BF* loses its superiority. The primary reason is with SNR kept constant, the power is spread out more evenly among the ray clusters and the power in the direction of the dominant ray decreases. Therefore, *Peak BF* and *Beamforming* performances decrease, but still outperform *Energy* detection.

Note that in Figs. 3-6, *Energy* detection curves for M=2 and M=4 remain relatively unchanged as the number of ray clusters increased. This behavior is caused by the non-uniformity of ray amplitudes. With non-uniform ray amplitudes, correlations between antennas are not very sensitive to increases in the number of ray clusters. Therefore, diversity gain only increases slightly as the number of ray clusters increases and the *Energy* detection curves in Figs. 3-6 remain relatively unchanged.

There are two key observations from Figs. 7-8. Firstly, using the statistical channel model, *Beamforming* detection does not give good results (*Peak BF* has no physical meaning and is not shown). This is because statistical models cannot account for propagation characteristics directly, especially the arrival angles. Secondly, as correlation decreases (or as diversity gain increases) between antennas, *Energy* detection performance increases. Since there is less correlation, even if one antenna does not give good results, other antennas may be able to compensate.

D. Complexity and Latency

With the ray-based channel model, *Peak BF* and *Beamforming* have superior performance over energy detection, but what are the drawbacks of implementing such detectors? Basically, there are no drawbacks. Note that the number of time samples required is the same for *E*nergy detection and both beamforming approaches. Thus, *Peak BF* is of the same computational complexity and latency as energy detection. *Beamforming* is twelve times that complexity and latency because twelve angles are tested. Even if the *Peak BF* is not applicable, the increase in computational time for *Beamforming* is still acceptable.

V. CONCLUSION

This paper has proposed a novel beamforming detection method to exploit propagation characteristics for spectrum sensing. Numerical results of a ray-based channel model at instantaneous power SNR equal to -20 dB for beamforming detection, either with prediction (*Peak BF*) or without prediction (*Beamforming*) of the dominant ray angle, has been shown to be superior to *Energy* detection. When a statistical channel model is employed, *Energy* detection performs better than *Beamforming*, because the statistical model does not capture the ray clustering propagation characteristic, especially the angles of arrivals. Since it is known from measurements that signals do arrive in clusters for a wide-range of communication scenarios (mobile-to-mobile, macro-cellular and micro-cellular), the use of a ray-based channel model results reflect the true physics in practice. The computational complexity and latency for *Peak BF* are the same as *Energy* detection, but increase slightly for *Beamforming*. Therefore, our proposed method is expected to provide the efficiency needed for practical implementations.

REFERENCES

[1] T. Yucek and H. Arslan, “A Survey of Spectrum Sensing Algorithms for Cognitive Radio Applications”; IEEE Communications Surveys & Tutorials; Vol. 11; No. 1; pp 116-130, 2009.

[2] Y. Zeng, Y. Liang, A. Hoang, and R. Zhang, “A Review on Spectrum Sensing for Cognitive Radio: Challenges and Solutions”; EURASI Journal on S. P.; Vol 2010; 2010

[3] W. A. Gardner, “Exploitation of spectral redundancy in cyclostationary signals,”; *IEEE Signal Processing Magazine*; vol. 8, no. 2, pp. 14–36, 1991.

[4] RH. Tang, “Some physical layer issues of wide-band cognitive radio systems,” in *Proc. IEEE Int. Symposium on New Frontiers in Dynamic Spectrum Access Networks*, Baltimore, Maryland, USA, Nov. 2005, pp. 151–159.

[5] Tandra and A. Sahai, “Fundamental limits on detection in low SNR under noise uncertainty,” in *Proceedings of the International Conference on Wireless Networks, Communications and Mobile Computing (WirelessCom '05)*, vol. 1, pp. 464–469, Maui, Hawaii, USA, June 2005

[6] A. Molisch, L. Greenstein, M. Shafi, “Propagation Issues For Cognitive Radio”; Proceeding of the IEEE; Vol. 97, No.5; May 2010

[7] Z. Quan, S. Cui, and A. H. Sayed, “Optimal linear cooperation for spectrum sensing in cognitive radio networks,” *IEEE Journal on Selected Topics in Signal Processing*, vol. 2, no. 1, pp. 28–40, 2007.

[8] R. Joong-Hyup Lee, Dong-Chan Oh, Yong-Hwan Lee, “Antenna Correlation Based Spectrum Sensing in Cognitive Radio Systems,” IEEE VTC 2010, Taipei

[9] Y. H. Zeng and Y.-C. Liang, “Spectrum-sensing algorithms for cognitive radio based on statistical covariances,” *IEEE Transactions on Vehicular Technology*, vol. 58, no. 4, pp. 1804–1815, 2009

[10] T. Taga, "Analysis for Mean Effective Gain of Mobile Antennas in Land Mobile Radio Environments", IEEE Trans., VT 39, May 1990, p. 117.

[11] J. Fuhl, J-P. Rossi and E. Bonek, "High-Resolution 3-D Direction-of-Arrival Determination for Urban Mobile Radio,” IEEE Trans. Ant. and Prop., vol. 45, pp. 672- 682, 1997.

[12] H.H. Xia, H.L. Bertoni, L.R. Maciel, A. Lindsy-Stewart and R. Rowe, "Radio Propagation Characteristics for Line-of-Sight Microcellular and Personal Communications"; IEEE Transactions on Antennas and Propagation; Vol. 41; No. 10; pp. 1439-1447, 1994.

[13] J. Lu, “Simplified Urban Propagation Models for Rapid Computation of Site-Specific Path Gain”; Master Thesis, Polytechnic Institute NYU, 2010 (Advisor: H.L. Bertoni).

[14] L. Piazzi and H.L. Bertoni, "Achievable Accuracy of Site Specific Path Loss Predictions in Residential Environments;" IEEE Trans. on Vehicular Technology; Vol. VT-48; No. 3; pp. 922-930, May 1999.

[15] K. Rizk, J-F. Wagen and F. Gardiol, “Two-Dimensional Ray-Tracing Modeling for Propagation Prediction in Microcellular Environments,” IEEE Transactions on Vehicular Technology; Vol. 46; No. 2; pp. 508-518, May 1997.

[16] K. Rizk, J.F. Wagen, J. Li and F. Gardiol, “Lamppost and panel scattering compared to building reflection and diffraction,” COST 259; May 1996

[17] D. Eppink, W. Kuebler, TIREM/SEM Handbook. Department of Defense Electromagnetic Compatibility Analysis Center, Annapolis, Maryland, 1994.

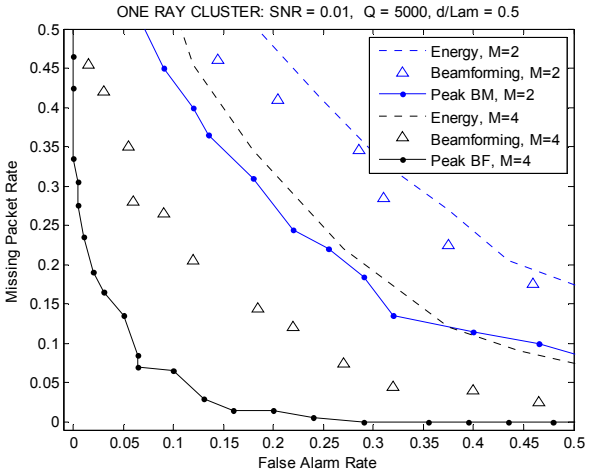

Fig. 3 One Ray Cluster

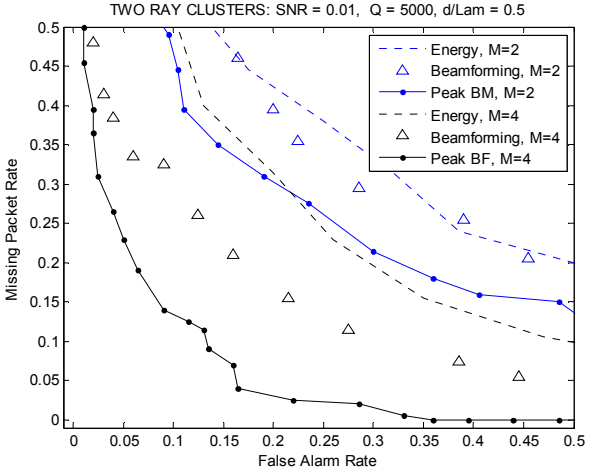

Fig. 4 Two Ray Clusters

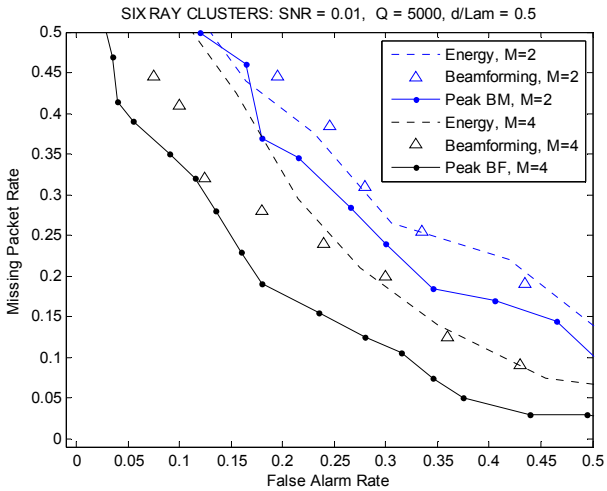

Fig. 5 Six Ray Clusters

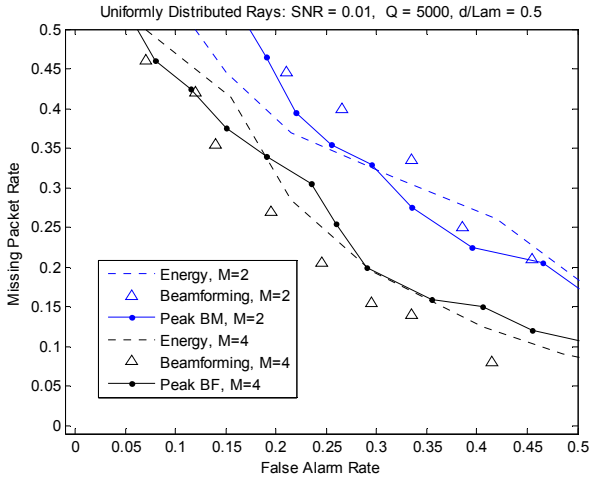

Fig. 6 Uniformly Arriving Rays

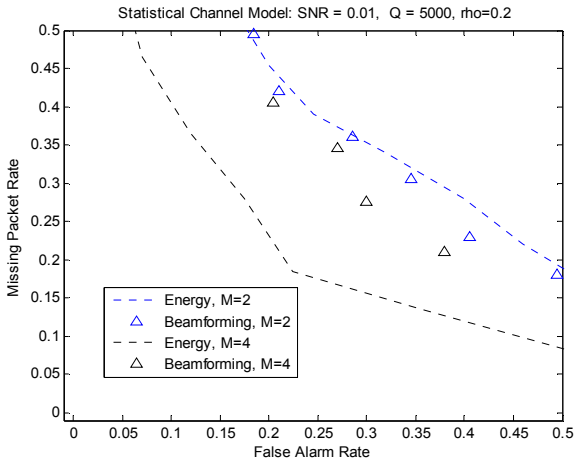

Fig. 7 Statistical Channel Model with $\rho = .2$

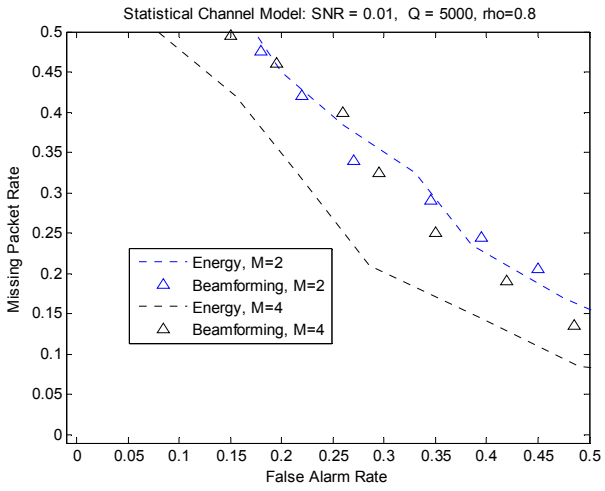

Fig. 8 Statistical Channel Model with $\rho = .8$